Catalysis Today 161 (2011) 255–259

Contents lists available at ScienceDirect

Catalysis Today

journal homepage: www.elsevier.com/locate/cattod

Structured catalysts for photo-Fenton oxidation of acetic acid

Diana Sannino[a,*], Vincenzo Vaiano[a], Paolo Ciambelli[a], Lyubov A. Isupova[b]

[a] *Department of Chemical and Food Engineering, University of Salerno, Via Ponte Don Melillo, 84084 Fisciano (SA), Italy*
[b] *Boreskov Institute of Catalysis, SB RAS, pr. Lavrentieva, 5, 630090 Novosibirsk, Russia*

ARTICLE INFO

Article history:
Received 23 June 2010
Received in revised form 14 October 2010
Accepted 7 November 2010
Available online 13 December 2010

Keywords:
Photo-Fenton oxidation
Heterogeneous process
Perovskites
Monolith

ABSTRACT

In this work photo-Fenton oxidation of acetic acid, was carried out on perovskites based structured catalysts, in the presence or in the absence of low amounts of Pt. Homogeneous photo-Fenton reaction by ferrioxalate complex has been also performed. The comparison of homogeneous and heterogeneous photo-Fenton oxidation indicates that the use of a heterogeneous structured catalyst greatly improves the total organic carbon (TOC) removal and leads to a more effective use of H_2O_2. The rate of TOC removal during the runtime decreased because of the occurring side H_2O_2 decomposition to O_2 that subtracts the oxidant to the photo-Fenton reaction. Moreover it allows enlarging the pH range of operation without the formation of sludge or significant metal leaching. $LaFeO_3$ and Pt/$LaMnO_3$ resulted the best catalysts for this process in terms of reaction rate.

1. Introduction

Advanced oxidation processes (AOPs) for the degradation of non-biodegradable organic contaminants in wastewater are very attractive alternatives to more traditional treatment techniques such as flocculation, precipitation, adsorption on granular activated carbon, air stripping or reverse osmosis [1,2]. AOPs usually operate at or near ambient temperature and pressure [3,4].

The free hydroxyl radicals ($^\bullet$OH) are primarily responsible for the efficiency of the AOPs. Its high oxidation potential in fact guarantees a rapid oxidation of the polluting molecules to CO_2. In both natural and drinking water, the average life-span of the $^\bullet$OH radicals is very short [5]. In fact, they attack the most part of organic molecules with rate constants usually in the order of 10^6–$10^9\,M^{-1}\,s^{-1}$ [6]. $^\bullet$OH radicals are also characterized by a little selectivity of attack which is a useful attribute for an oxidant used in wastewater treatment for solving pollution problems. The versatility of AOPs is also enhanced by the fact that they offer different possible ways for the production of $^\bullet$OH radicals thus allowing a better compliance with the specific treatment requirements [7].

A known method to reduce the pollutant concentration in effluent wastewater, is the Fenton process which involves the addition of hydrogen peroxide (H_2O_2) and Fe(II) compounds to wastewater so that the organic pollutants are oxidized by the hydroxyl free radicals ($^\bullet$OH) produced by the reaction between hydrogen peroxide and the ferrous ion. However, the Fenton-like method is not completely satisfactory since the overall oxidation rate is slowed down after conversion of Fe^{2+} to Fe^{3+} due to slower reduction of Fe^{3+} back to Fe^{2+}. In order to overcome this problem, the application of UV–visible irradiation of the Fenton reaction system, resulting in the so-called photo-assisted Fenton reaction (or photo-Fenton system), regenerates ferrous ions (Fe^{2+}) by photolysis of hydroxide complexes of Fe^{3+}, yielding additional hydroxyl radicals. This last system is expected to be an efficient method for wastewater treatment [8–13]. Drawbacks due to the application of homogeneous catalysts, such as limited pH range, production of Fe containing sludge, and deactivation [14] could be overcome by heterogeneous catalytic systems. Various studies have been carried out on the heterogeneous photo-Fenton system; in particular, Fe over HY zeolite has been used for the degradation of polyvinyl alcohol [15]. The immobilization of Fe ions also on clays, bentonite and laponite for the oxidation of the azo dye Orange II has been reported [16]. Similar works have been also described for the degradation of different azo-dyes over iron oxides such as goethite and hematite under non-controlled pH conditions [17]. Nafion has been employed as organic support due to the presence of sulphonic groups allowing the effective anchoring of Fe ions [18]. Photo-Fenton oxidation of phenol was also performed using iron species incorporated over different silica supports [19].

Heterogeneous Fe(III) based photo-Fenton catalyst is often used as suspended particles in the liquid reaction medium [20]. Thus the biggest disadvantage lies in the fact that, after wastewater treatment, separation of catalyst from reaction solution is needed. To avoid this last operation the use of structured catalysts could be a valid solution. Recently, we have reported an innovative application of monolith structured catalysts in heterogeneous photo-Fenton process [21,22].

---

* Corresponding author. Tel.: +39 089964147; fax: +39 089964057.
E-mail address: dsannino@unisa.it (D. Sannino).

0920-5861/$ – see front matter © 2010 Elsevier B.V. All rights reserved.
doi:10.1016/j.cattod.2010.11.025

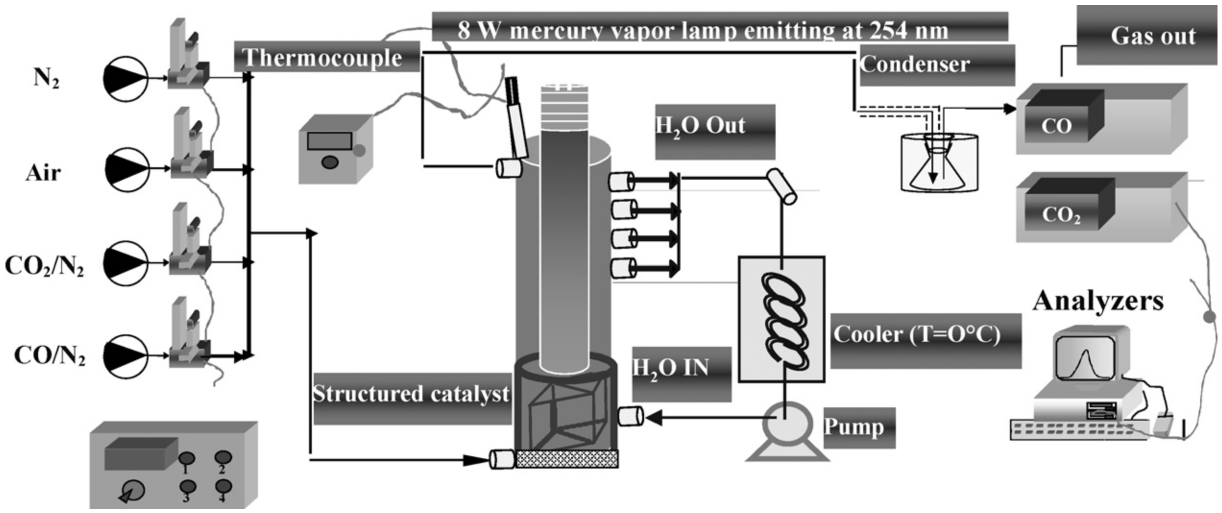

Fig. 1. Laboratory apparatus for the catalytic photo-Fenton oxidation.

In this work photo-Fenton oxidation of acetic acid, chosen as model pollutant, was carried out on Fe-, Mn-, Co-, Ni-, Cu-based perovskites supported on cordierite monolith, in the presence or in the absence of low amounts of Pt. Homogeneous photo-Fenton reaction by ferrioxalate complex has been also performed for comparison. The influence of perovskite loading and pH values was investigated.

2. Experimental

2.1. Structured catalysts preparation and characterization

The honeycomb cordierite support was made by the extrusion of plastic paste (prepared from a talc, a clay, alumina ($Al_2O_3 \cdot nH_2O$) taken in a required ratio and ethylene glycol water solution) followed by drying and calcination at 1160 °C for 4 h.

Supported perovskites $LaMeO_3$ (Me = Mn, Co, Fe, Ni, Cu) were prepared by impregnation of thin wall (wall thickness ~0.4 mm) of monolithic honeycomb cordierite support with triangular channels ~2.5 mm, specific surface area ~2 m^2/g and total/overall pore volume ~0.2 cm^3/g. Solutions of nitrate salts in the ethylene glycol with added citric acid were used. After drying at 100–200 °C, a film of polymerized metal–ether complexes strongly adhering to the monolithic support walls is formed. After annealing at temperatures exceeding 500 °C, the organic residue is burned, and grainy porous perovskite supported layer emerges. The typical procedure is reported in [23]. Samples were calcined in air at 900 °C for 4 h. Pt metal (=0.1 wt%) was supported by wet impregnation from H_2PtCl_6 on the cordierite substrate which were either pure or precovered by the oxide sublayer. After Pt loading, samples were either directly dried under air or, before drying, treated with hydrazine hydrate.

$Fe_2(C_2O_4)_3$ (provided by Carlo Erba) was chosen as the reference homogeneous photo-Fenton catalyst.

The structural and textural characteristics of supported perovskites were studied by XRD, SEM, X-ray microanalysis, thermal analysis and adsorption measurements as reported in [23].

The X-ray diffraction patterns were obtained with a URD-6 diffractometer using CuKα-radiation. The 2θ scan region was 10–70°. Typical particle sizes were estimated from the broadening of 400 diffraction peak (cubic index) not split due to the hexagonal distortion of the perovskite structure.

The samples pore structure was characterized by the high pressure mercury porosimetry (HPM) using an Auto-Pore 9200 equipment, and the specific surface area was determined by a routine BET procedure using the Ar thermal desorption data.

2.2. Photo-Fenton oxidation tests

Photo-Fenton tests were carried out on 160 ml of solution in a properly designed sealed stainless-steel batch photoreactor [24]. Model aqueous solutions containing an initial concentration of acetic acid, expressed as total organic carbon (TOC), and H_2O_2 equal to 500 mg/l (0.021 mol/l) and 0.083 mol/l, respectively, at pH 3.9 were used in the typical tests. An 8 W mercury vapor lamp emitting at 254 nm and the monolith catalysts were placed along the reactor axis. When the lamp was switched on, the reaction started. Small amounts of samples of treated solution (500 μl) were taken for analyses every hour, to avoid changing in the contact time during the test.

The total organic carbon (TOC) has been determined by the high temperature catalytic combustion method in a specifically developed equipment, using a Pt/Al_2O_3 catalyst in a tubular flow reactor operating at 680 °C. High purity grade air was fed to the catalytic reactor for the combustion, with a gas flow rate of 250 ml/min (STP). A specifically developed and heated injection system was used for liquid sample vaporization and transfer. In particular, the injection of a fixed volume of the solution (100 μl) was realized by means of a microliter syringe (Hamilton), with a pneumatic system at pressure $P = 2$ bar, in the heated line ($T = 170$ °C) before the reactor. Combustion products were monitored by NDIR continuous analyser (Hartmann & Braun Uras 10E), measuring CO and CO_2 gaseous concentrations at the combustion reactor outlet, and a paramagnetic analyser (Hartmann & Braun Magnos 6G) for continuous monitoring of O_2 concentration. Finally, the signals from the analysers are acquired and processed by personal computer. Both CO and CO_2 concentration continuous data were jointly integrated to calculate total organic carbon. The H_2O_2 concentration was determined by $H_2O_2/TiOSO_4$ complex ($\lambda = 405$ nm) UV–vis analyses. A schematic picture of the laboratory apparatus for photo-Fenton tests is reported in Fig. 1. Continuous mixing of model wastewaters was realized by nitrogen fine bubbling under monolith holder ($Q = 250$ ml/min (STP)) and external recirculation of wastewater (flow rate = 7 l/min). Before re-entering into the reactor the solution was cooled by a cold trap to keep the temperature constant at 25 °C. At the reactor outlet the gases pass through a cold trap (0 °C) in order to assure water condensation, prior to the gas analyser (Quantra Fourier transform ion cyclotron resonance mass spectrometer, Siemens) for measurements of CO and CO_2 concentrations. The catalytic properties of monolithic samples were tested in the photo-Fenton reaction under atmospheric pressure at 25 °C using samples mass comprised between 1.5 and 6.4 g.

Table 1
Catalysts and their characteristics.

Perovskite catalyst	Active phase loading (wt%)
$LaMnO_3$	2.69
2-$LaFeO_3$	2.24
5-$LaFeO_3$	4.9
10-$LaFeO_3$	10.5
$LaNiO_3$	2.52
$LaCoO_3$	2.94
$LaCuO_3$	2.66
Pt/$LaMnO_3$	2.69

Leaching tests were carried out to check the potential of leaching of the metals from the perovskite during the catalytic tests, analysing the solution by ICP-AES (Varian Liberty II). This method allowed direct determination of the presence of metal ions in solution.

3. Results and discussion

3.1. Structured catalysts characterization

The list of heterogeneous catalysts tested in the photo-Fenton oxidation with the active phase loading is reported in Table 1. The specific surface area of all the samples was about 1 m^2/g. The pore size distribution (not reported) and the total pore volume were about 0.2 cm^3/g, and resulted similar for all the samples. This assured that the catalytic performances of the different supported perovskites catalysts are not dependent on different diffusional effects.

X-ray diffraction results are reported in Fig. 2. The mixtures of cordierite and perovskite phases were observed for all the samples. For supported lanthanum manganites and ferrites, the type of structure is hexagonal and orthorhombic, respectively, as previously found [23].

In the case of cuprates, nickelates and cobaltites, instead of a stable hexagonal phase, a cubic modification was revealed due to an interaction between the active component and support [23].

3.2. Photo-Fenton oxidation tests

Preliminary results carried out in the absence of UV irradiation showed that the efficiency of Fenton oxidation of acetic acid on perovskites based catalysts is very low with a maximum TOC removal of 8% after 4 h of reaction time [24].

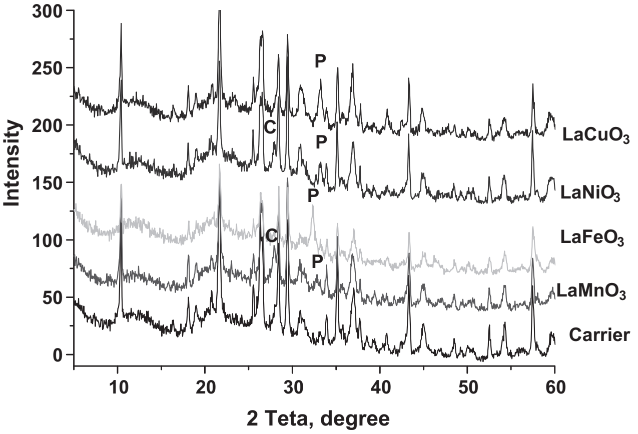

Fig. 2. X-ray diffraction patterns of cordierite carrier and supported catalysts. P: perovskite peaks, C: lanthanum oxy-carbonate peaks.

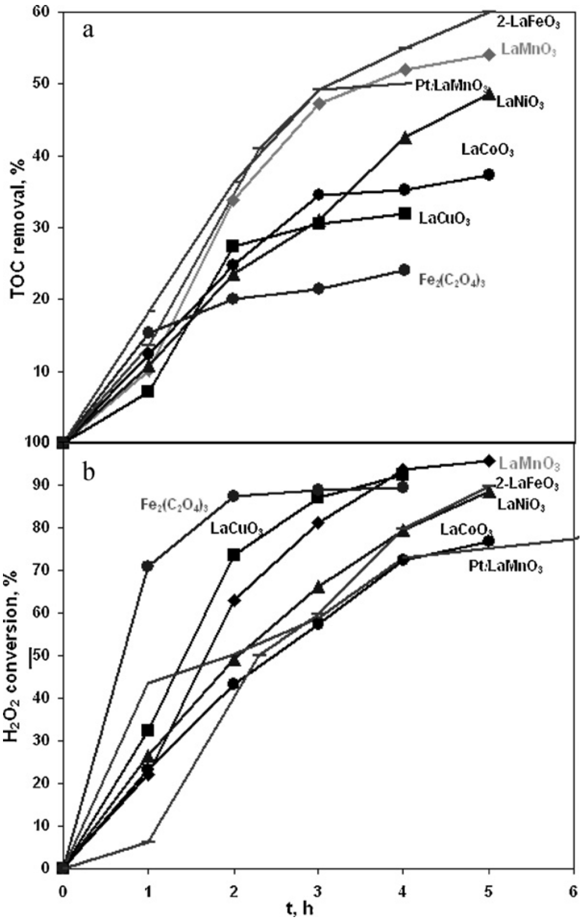

Fig. 3. TOC removal (a) and H_2O_2 conversion (b) as a function of reaction time; initial pH of the solution: 3.9.

For photo-Fenton oxidation tests, at the run starting time, the nitrogen stream was passed through the reactor in the absence of irradiation at ambient temperature for $t = 10$ min and then the UV lamp was switched on. For all the catalysts, the analysis of the gas evolved during runtime from the sealed photoreactor allowed to evidence the presence of only CO_2 as product. The total carbon mass balance, evaluated from the values of TOC removal and carbon dioxide amount evolved in gas phase, was closed to about 98%. This indicates that complete mineralization of acetic acid was obtained in photo-Fenton oxidation [24].

Fig. 3a and b, shows, respectively, TOC removal and H_2O_2 conversion for heterogeneous photo-Fenton in comparison with homogeneous reaction. Heterogeneous catalysts showed higher TOC removal efficiency, despite the fact that the homogeneous catalyst was faster in a shorter reaction time. In fact, the Fe^{2+} activity appeared to decrease after one hour of irradiation reaching the lower final degree of TOC reduction with respect to heterogeneous perovskites because of the very high H_2O_2 consumption. Thus, for longer time, the heterogeneous catalysts showed higher TOC removal efficiency with lower H_2O_2 consumption.

The TOC removal after 5 h reached the value of 60, 54 49, 50, 37 and 32% for 2-$LaFeO_3$, $LaMnO_3$, $LaNiO_3$, Pt/$LaMnO_3$, $LaCoO_3$ and $LaCuO_3$, respectively. The addition of Pt enhanced the initial rate of acetic acid removal.

However, Pt presence did not significantly enhance catalytic performance after five hours although on Pt/$LaMnO_3$ catalyst the value of TOC reduction after one hour of irradiation was the highest for all the catalysts (about 18%).

Table 2
Reaction rate for heterogeneous process after one hour of reaction time.

Perovskite catalyst	Initial TOC removal rate $(\text{mmol h}^{-1}\ \text{g}_{\text{gactive phase}}{}^{-1})$
$LaMnO_3$	2.6
2-$LaFeO_3$	4.6
$LaNiO_3$	2.4
$LaCoO_3$	2.6
$LaCuO_3$	1.4
Pt/$LaMnO_3$	3.8

Table 3
TOC removal after one hour of irradiation as a function of perovskite loading; catalyst weight: 1.5 g.

Perovskite catalyst	Perovskite loading (wt%)	TOC removal after 1 h of irradiation (%)
2-$LaFeO_3$	2.24	6.8
5-$LaFeO_3$	4.9	16.4
10-$LaFeO_3$	10.5	31.1

Considering that differential reaction conditions are so far found after 1 h, since TOC conversions were below 20%, the initial TOC removal rate referred to the mass of active perovskite phase was evaluated and reported in Table 2. The catalytic performances of $LaMnO_3$ monolith were improved by Pt addition. However, both higher initial rate of TOC removal and higher final extent of acetic acid conversion were observed with $LaFeO_3$. The scale of activity was: $LaFeO_3 > Pt/LaMnO_3 > LaCoO_3 \approx LaNiO_3 > LaMnO_3 > LaCuO_3$.

Photo-Fenton oxidation experiments have also been performed on powder catalysts in order to evaluate the presence of diffusive phenomena. A test was performed on supported $LaMnO_3$ monolith powdered in an agate grinder.

Fig. 4 shows higher TOC removal (about 55%) on the monolith with respect to the grinded monolith (about 43%) with H_2O_2 consumption of 100% after 4 h, although after 1 h TOC removal is higher for the powdered monolith. A second experiment was performed using bulk perovskite powder in a similar amount to that present on the monolith piece, i.e. by considering 2.69 wt% of the supported perovskites on a monolith fragment of 6.0 g, it was evaluated that 0.184 g of powder bulk $LaMnO_3$ have to be employed. The obtained results (Fig. 4) evidenced higher TOC removal (about 55%) for the monolith with respect to the bulk perovskite (about 52%) when H_2O_2 consumption of 100% is achieved. Considering these last results, it is evident that photo-Fenton heterogeneous activity resulted unaffected by diffusional limitations; the effected tests proceeded in chemical regime and photoactivity is to be ascribed to the perovskite phase as the active phase where the reaction takes place.

$LaFeO_3$ based catalysts were chosen to investigate the effect of active phase washcoat load. The obtained results are summarized in Table 3. TOC removal after 1 h of reaction time increased from 6.8 to about 31% with increase of perovskite load from 2.2 to 10.5 wt%. These results clearly indicate that photo-Fenton activity is closely related to the amount of active phase supported on monolith carrier.

According to other studies [25,26], pH is one of the key parameters influencing the rate of degradation of organic pollutants in photocatalytic processes and it is also an important operational variable in wastewater treatment systems. Since the highest performances were obtained on 10-$LaFeO_3$ catalyst, the effect of initial pH of the solution was studied on this latter catalytic system in the pH range of 3.9–8 (Fig. 5).

By increasing the pH from 3.9 to 6, TOC removal increased from about 24 to 57%, while at pH = 8 TOC removal decreased to 46% after 4 h of reaction time. At pH = 6, the H_2O_2 conversion reached the value of 100% after 5 h and at fixed reaction time was lower than at pH = 3.9. Finally, in more basic conditions its decomposition was faster and complete after 3 h.

The results of leaching test showed that Fe concentration in the treated solutions after photo-Fenton tests is very low, 0.55, 0.33 and 2.45 mg/l at pH = 3.9, 6 and 8 respectively, indicating an acceptable or negligible metal dissolution from the heterogeneized $LaFeO_3$ during acetic acid photo-oxidation for all the pH conditions. Sludge formation was never observed.

The data of H_2O_2 conversion (Figs. 3 and 5) suggest that the rate of TOC removal by photo-Fenton oxidation decreased because of H_2O_2 decomposition to O_2, which subtracts the oxidant to the photo-Fenton reaction. Two main competitive reactions could be advised in the photo-Fenton system, according to the following:

$$CH_3COOH + 4H_2O_2 \rightarrow 2CO_2 + 6H_2O \tag{1}$$

$$H_2O_2 \rightarrow H_2O + \frac{1}{2}O_2 \tag{2}$$

To overcome this problem, a gradual addition of H_2O_2 could be performed by adding small volumes of concentrated solution of H_2O_2 each hour. Moreover, it is worthwhile to take into account that, in order to make the photo-Fenton process competitive with other AOPs, it is crucial to have low operation costs, which nec-

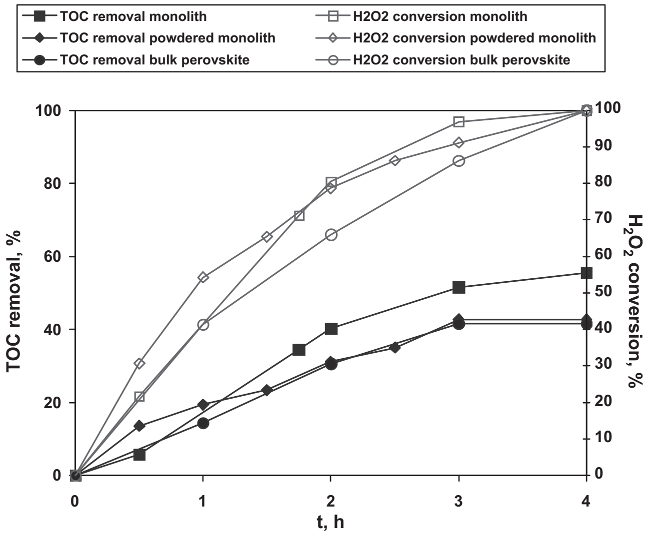

Fig. 4. Comparison of photo-Fenton activity of the $LaMnO_3$ monolith with respect to powdered catalyst and bulk perovskite; initial pH of the solution: 3.9.

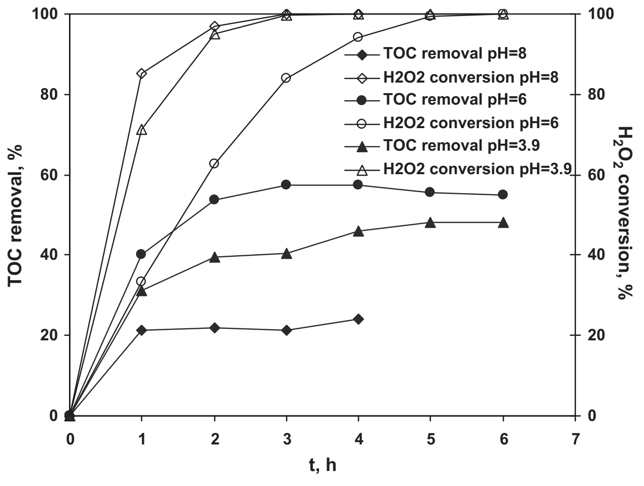

Fig. 5. Effect of pH on the catalytic activity of 10-$LaFeO_3$.

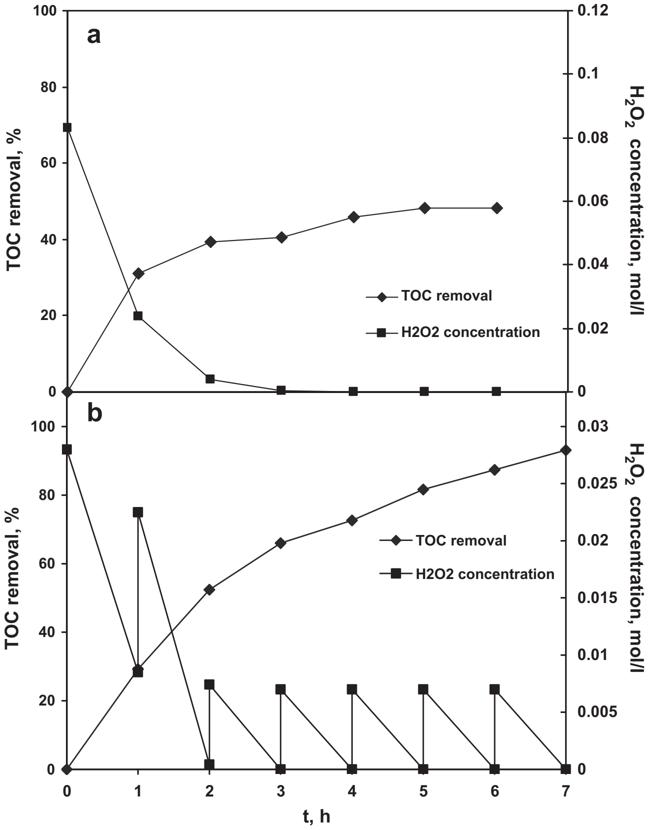

Fig. 6. Photo-Fenton oxidation on 10-$LaFeO_3$ without H_2O_2 dosage (a) and with H_2O_2 dosage (b); initial pH of the solution: 3.9.

essarily imply to have low consumption of H_2O_2. A controlled concentration of H_2O_2 could permit higher TOC reductions in shorter times, limiting the scavenger effect of H_2O_2 that traps highly reactive hydroxyl radicals produced by photolysis [27,28], highlighting the need to perform the reaction with an adjusted concentration of H_2O_2 during all the reaction time.

The influence of H_2O_2 dosage on TOC removal was investigated for 10-$LaFeO_3$ catalyst and the results are reported in Fig. 6.

Without H_2O_2 dosage (Fig. 6a) about 46% of TOC removal was obtained after 4 h, when a total H_2O_2 consumption was achieved. The trend of H_2O_2 concentration with its dosage into the reactor (Fig. 6b) resulted in a saw tooth profile. It is worthwhile that a variable addition of H_2O_2 (0.014 M/h after 1 h and 0.007 M/h during the remaining irradiation time) increased the TOC removal up to 93% after 7 h.

By evaluating the specific H_2O_2 consumption at the maximum TOC removal obtained in each test as $\mathrm{mol}_{H_2O_2}/\mathrm{mol}_C$, it is found equal to 4.15 mol/mol (7.33 $g_{H_2O_2}/g_C$) in the test without dosage while results 2.15 $\mathrm{mol}_{H_2O_2}/\mathrm{mol}_C$, by step H_2O_2 addition, closest value to molar ratio H_2O_2/C in the reaction (1) alone.

In summary, the step addition of H_2O_2 during the photo-Fenton reaction ensures the fruitful utilization of the produced hydroxyl radicals for the acetic acid oxidation reaction. Tests (not reported) in the presence or in the absence of UV light, perovskite, acetic acid, H_2O_2 and catalyst characterization after photo-Fenton tests, suggest a different path for the oxidation reaction, involving the adsorption and activation of hydrocarbon on perovskites, formation of $^{\bullet}OH$ radicals from H_2O_2 photolysis, and the oxidation of adsorbed hydrocarbon species by the UV generated hydroxyls radicals which regenerate the catalyst surface. Further studies are in progress.

4. Conclusions

The comparison of homogeneous and heterogeneous photo-Fenton oxidation indicates that the use of a heterogeneous structured catalyst greatly improves TOC removal and leads to a more effective use of H_2O_2. Moreover it allows enlarging the pH range of operation without formation of sludge or metal leaching. $LaFeO_3$ and Pt/$LaMnO_3$ are resulted the best catalysts for this process in terms of reaction rate. Photo-Fenton activity is closely related to the amount of active phase supported on monolith carrier. The rate of TOC removal decreases because of the occurring side H_2O_2 decomposition to O_2 that subtracts the oxidant to the photo-Fenton reaction. This problem is overcome by adding H_2O_2 during the photo-Fenton reaction allowing to enhance strongly the TOC removal.

Acknowledgment

The authors thank Eng. Daniela Caracciolo and Research Institute of Leather Industry (SSIP) of Naples (Italy) for making leaching tests.

References

[1] O. Legrini, E. Oliveros, A.M. Braun, Chem. Rev. 93 (1993) 671.
[2] R. Bauer, G. Waldner, H. Fallmann, S. Hager, M. Klare, T. Krutzler, S. Malato, P. Maletzky, Catal. Today 53 (1999) 131.
[3] W.H. Glaze, J.W. Kang, D.H. Chapin, Ozone Sci. Eng. 9 (1987) 335.
[4] E.M. Aieta, K.M. Regan, J.S. Lang, L. McReynolds, J.W. Kang, W.H. Glaze, J. AWWA 80 (1988) 64.
[5] C. Caretti, C. Lubello, Water Res. 37 (2003) 2365.
[6] J. Hoigné, H. Bader, Water Res. 17 (1983) 185.
[7] R. Andreozzi, V. Caprio, A. Insola, R. Marotta, Catal. Today 53 (1999) 51.
[8] K. Hislop, K.J. Bolton, Environ. Sci. Technol. 33 (1999) 3119.
[9] M. Trapido, J. Kallas, Environ. Technol. 21 (2000) 799.
[10] J. Vicente, R. Rosal, M. Diaz, Ind. Eng. Chem. Res. 41 (2002) 46.
[11] V. Kavitha, K. Palanivelu, Chemosphere, 55 (2004) 1235.
[12] J. Farias, E.D. Albizzati, O.M. Alfano, Ind. Eng. Chem. Res. 49 (2010) 1265.
[13] G. Li Puma, P.L. Yue, Proceedings at the Sixth International Conference on Advanced Oxidation Technologies for Water and Air Remediation, London, Ontario, Canada, June 26–30, 2000, p. 105.
[14] E.V. Kuznetsov, E.N. Savinov, L.A. Vostrikova, V.N. Parmon, Appl. Catal. B: Environ. 51 (2004) 165.
[15] S.H. Bossmann, E. Oliveros, S. Gob, M. Kantor, A. Goppert, L. You, P.L. Yue, A.M. Braun, Water Sci. Technol. 44 (2001) 257.
[16] J. Feng, X. Hu, P.L. Yue, Water Res. 39 (2005) 89.
[17] J. He, X. Tao, W. Ma, J. Zhao, Chem. Lett. (2002) 86.
[18] J. Fernandez, J. Bandara, A. Lopez, P. Buffat, J. Kiwi, Langmuir 15 (1999) 185.
[19] F. Martınez, G. Calleja, J.A. Melero, R. Molina, Appl. Catal. B: Environ. 70 (2007) 452.
[20] S. Bossmann, E. Oliveros, S. Gob, S. Siegwart, E. Dahlen, L. Payawan, M. Straub, M. Worner, A. Braun, J. Phys. Chem. 102 (1998) 5542.
[21] D. Sannino, P. Ciambelli, M. Ricciardi, L. A. Isupova, PCT application, WO2008IT00343 20080523.
[22] D. Sannino, P. Ciambelli, M. Ricciardi, L.A. Isupova, Catalyst and heterogeneous photocatalytic Fenton process for sewage treatment, Russian patent RU2347611, February 27, 2009; Italian patent application, SA2008/A000012, May 29, 2007.
[23] L.A. Isupova, E.F. Sutormina, N.A. Kulikovskaya, L.M. Plyasova, N.A. Rudina, I.A. Ovsyannikova, I.A. Zolotarskii, V.A. Sadykov, Catal. Today 105 (2005) 429.
[24] M. Ricciardi, Wastewater treatment by high efficiency heterogeneous photo-Fenton process, PhD Thesis, University of Salerno, 2007.
[25] H. Gupta, S. Tanaka, Water Sci. Technol. 31 (1995) 47.
[26] C. Canton, S. Esplugas, J. Casado, Appl. Catal. B: Environ. 43 (2003) 139.
[27] R. Alnaizy, A. Akgerman, Adv. Environ. Res. 4 (2000) 233.
[28] M.Y. Ghaly, G. H¨artel, R. Mayer, R. Maseneder, Waste Manage. 21 (2001) 41.